Hardware Report

Cable-Monitor

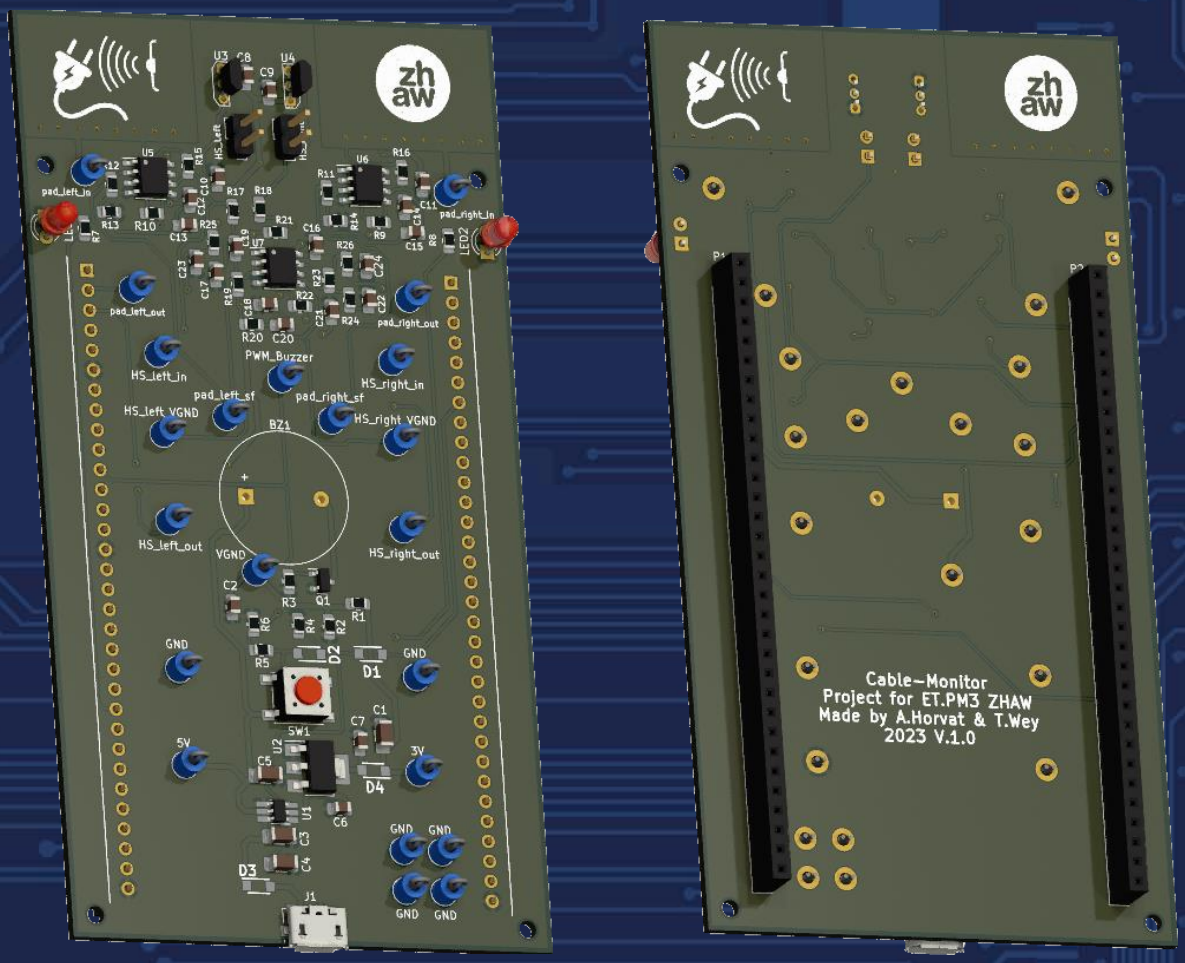

Authors: Alejandro Horvat & Timo Wey

Institute: ZHAW

Lecturers: Andreas Ehrensperger & Igor Matic

Subject: Project Module 3

Date: 20 October 2023

Abstract

As part of the Project Module 3 in the 5th Semester, the objective was to develop a Cable-Monitor. This device should be able to find hidden cables in walls, floors and ceilings by measuring the electromagnetic and electrostatic fields of the cable. By making use of the display from the provided development kit, the user is guided to the approximate location of the cable. In addition, audible feedback is provided using a buzzer and useful information such as the current and voltage, is shown on the display. To be able to measure such weak signals, an amplifier had to be used. The amplification was also paired with a Multi-Feedback-Bandpass-Filter (MFB) to eliminate unnecessary frequencies and filter out the wanted 50 Hz signal. Subsequently, the signal is fed into an Analog-to-Digital-Converter (ADC) and read by the microcontroller. The final product aims to detect various types of cables, including one- or two-phased cables and will feature an intuitive touch interface. The challenge extended beyond the realms of hardware and software to effective teamwork, as the project was a collaborative effort between two individuals. Successful completion required meticulous planning and coordination between team members.

Table of Contents

1. Introduction

This hardware report provides a comprehensive documentation of the Cable-Monitor hardware, covering specifications, evaluation, development/implementation, testing and project management. Facilitated by the provision of various documents, such as documentation templates, circuit designs, layouts, and program code frameworks, the project's initiation took place. The primary objective is the successful creation of a functional device capable of sensing a power cable through both electrostatic and electromagnetic fields. As a result, the device has been engineered to measure the distance to the cable and accurately gauge the current flowing through it. Acquired data is then presented on a touch display. Ultimately, the report aims to capture the entire lifecycle of the Cable-Monitor project, from conceptualization to realization, ensuring a clear understanding of the processes involved in achieving a fully operational and effective device.

2. Hardware specifications

The Cable-Monitor hardware must meet the following requirements:

- Detect a mains cable at a distance of up to 200 mm
    - Filter and amplify electrical field and frequency (50 Hz) of the mains cable
- Detect the electromagnetic field of the mains cable
    - Filter and amplify the electromagnetic field and frequency (50 Hz) of the mains cable
- Battery powered, preferably with automatic shut down when not in use
- Layout must be compatible for use with STM32F429 Discovery board

Additionally, the following software requirements should also be fulfilled:

- Display the distance to the cable in the range from 5mm to 100mm with a precision of ± 30%
- Display the angle to the cable in the range of ± 45° with a precision of ± 15°
- Menu with these items
    - Start single measurement
    - Start accurate measurement (averaging: mean and standard deviation)

Note: This document does not cover the software aspects of this project.

(Hochreutener, 2023)

The following additional features have also been implemented in the hardware design:

- External power supply to completely power on/off the device
    - Addition of a power on/off button that can also be read by the microcontroller
- LEDs to help the user navigate the direction of the mains cable
- Buzzer to provide audible feedback on mains cable location

3. Evaluation

The specifications and templates have almost finalised the main board design in a piggyback style. This design allows the board to be connected directly to the microcontroller board using the header pins of the STM32F429 Discovery board, resulting in a very compact footprint. An alternative would have been to create an external board connected to the microcontroller board by cables. However, this design choice would have increased the overall footprint and made the setup cumbersome to use. In addition, the lack of a template for this design style would have unnecessarily complicated and slowed down the entire layout process. The piggyback style was chosen because it provides a simple and elegant solution for connecting both the cable monitor board and the microcontroller board.

There are only a handful of sensor variants available for measuring electric and electromagnetic fields. The electrostatic field can only be measured using pads, while the electromagnetic field can be measured using a coil or a Hall sensor (see Figure 1). Both give similar output signals, but the coil requires additional circuitry to sense the fields. The hall sensor was therefore chosen.

Both sensors require additional amplification and filtering circuitry, as illustrated in Figure 1. It is essential to introduce a virtual ground to counterbalance the negative voltages of the sensor signals. This adjustment ensures that the ADC input of the microcontroller can accurately interpret the signal.

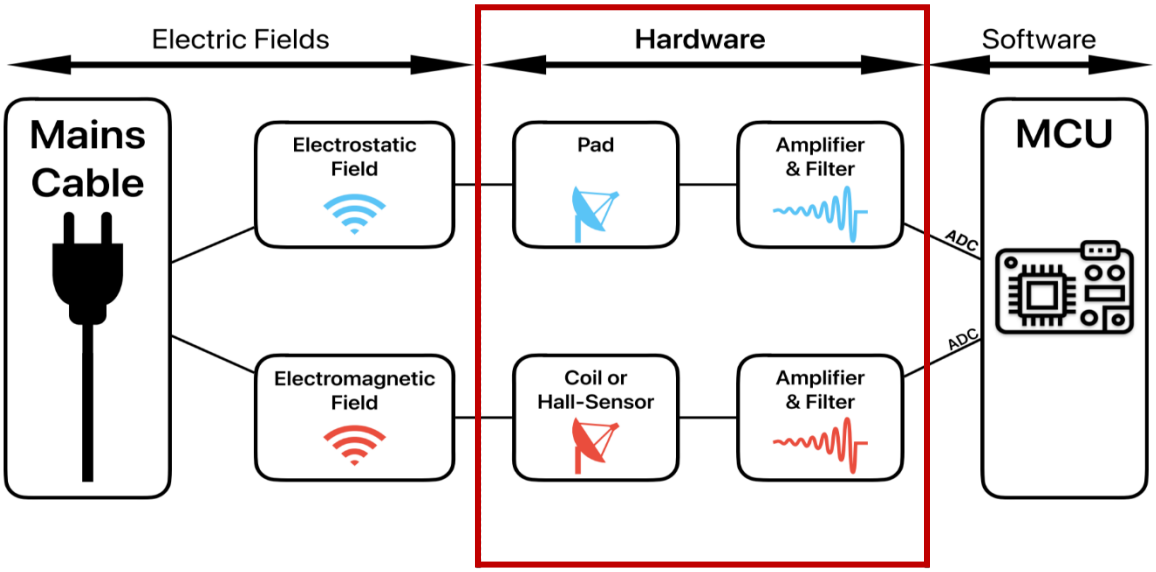

Figure 1: Block diagram of Cable-Monitor board

As the pads are more susceptible to interference and stray fields, the following amplification and filtering options were considered:

1. One amplifier with a multiple feedback band-pass filter (2nd order) with a virtual ground
2. One amplifier with a multiple feedback low-pass filter (2nd order) with a virtual ground
3. One amplifier with a simple low-pass filter (1st order) with a virtual ground

Only single amplifier options were considered to decrease power consumption and expenses. Variant three possesses a lower cut-off frequency, rendering variants one and two more appropriate. As only a single frequency range (50Hz) was sought, the implementation of a bandpass filter (variant 1) enabled the omission of undesired frequencies and decreased the amount of digital filtering overhead required. In contrast to variant 1, variant 2 would necessitate more digital filtering. Variant one was thus selected.

The hall sensor is significantly less susceptible to stray magnetic fields and interference. Therefore, a basic low pass filter and amplifier with a virtual ground proved adequate.

4. Development

4.1. Circuit designs

4.1.1. Power Supply

All power supply components were chosen because they were either included in the template or readily available in a KiCad library, as well as being in stock in ZHAW's inventory. Decoupling capacitors were selected in accordance with the suggested values from the datasheets. For added safety and to prevent any stray currents from flowing back from the power sources, Shottky diodes were added to all power supplies.

To allow the microcontroller to read the on/off switch (PE3), a voltage divider was incorporated as shown in Figure 2, upper right circuit. This calculation proves necessary as the switch requires 5 V from the power source, while the microcontroller's input pin can only accommodate voltages up to 3 V. Therefore the subsequent voltage divider was calculated:

$$V_{PE3} = \frac{5\ V}{R_5 + R_6} * R_6 = \frac{5\ V}{30\ k\Omega + 43\ k\Omega} * 43\ k\Omega = 2.945\ V\ \approx 3\ V \qquad (1)$$

An additional capacitor was added to the on/off circuit to keep the 5 V voltage long enough so that the micro controller can turn on and latch itself on. The Value was roughly chosen with 100 µF.

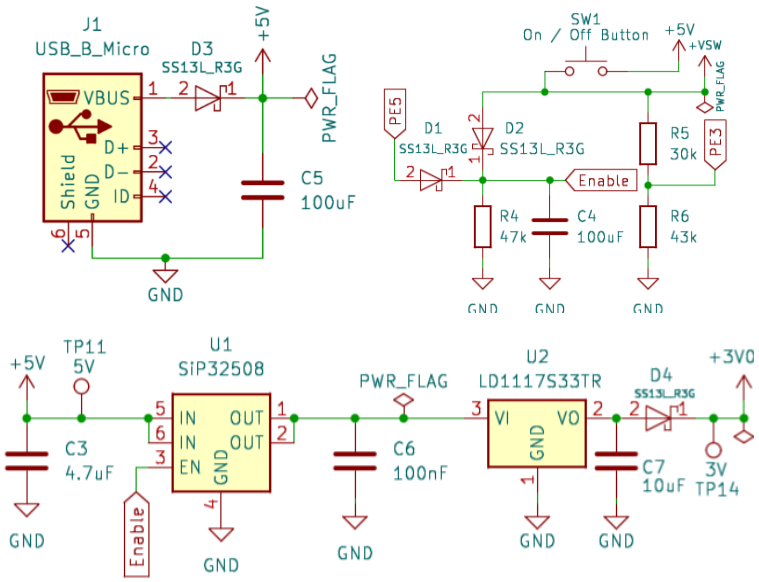

Figure 2: Power Supply Input, On-Off Circuit and Load-Switch with DC/DC converter

4.1.2. Virtual Ground

The virtual ground, established by a simple voltage divider comprising two resistors, aims to achieve the desired voltage of 1.5 V (refer to formula 1 for a similar calculation). To maintain low power consumption while ensuring sufficient current to stabilize the voltage, a recommended value of 10 kΩ was employed. To decouple the voltage, a 220 nF capacitor was utilized, which was also readily available in the template.

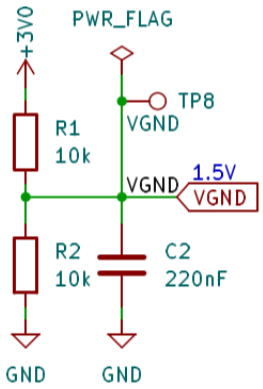

Figure 3: Virtual Ground circuit

4.1.3. Additional features

To accommodate the buzzer's requirement for higher voltages than the microcontroller can provide, a transistor was introduced. The transistor type and resistor value were specified in the template (refer to Figure 4, left circuit). The buzzer can be modulated by a PWM signal originating from the microcontroller.

In order to achieve optimal brightness for the directional LEDs with the microcontroller's output voltage, a resistor with an appropriate value had to be incorporated (refer to Figure 4, right circuit).

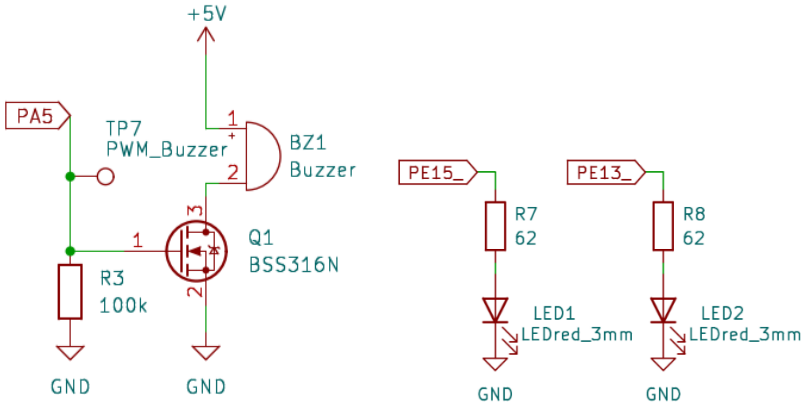

Figure 4: Circuit for Buzzer and directional LEDs

4.2. Electrostatic field

This section describes how the wire-to-pad capacitance was calculated using the provided MATLAB script E_B_Field.m (Appendix C). The script is designed for square pads, thus the approximate length x had to be calculated first:

$$x = \sqrt{l \cdot b} = \sqrt{22{,}86\ mm \cdot 15{,}62\ mm} = 19{,}89\ mm \tag{2}$$

The result is then further used to determine the wire-to-pad capacitance using the provided MATLAB-Script E_B_Field.m (Appendix C). At 5 mm a capacitance of approximately 0.37 pF was chosen. This value was chosen at that distance to reduce overdrive but maximize gain.

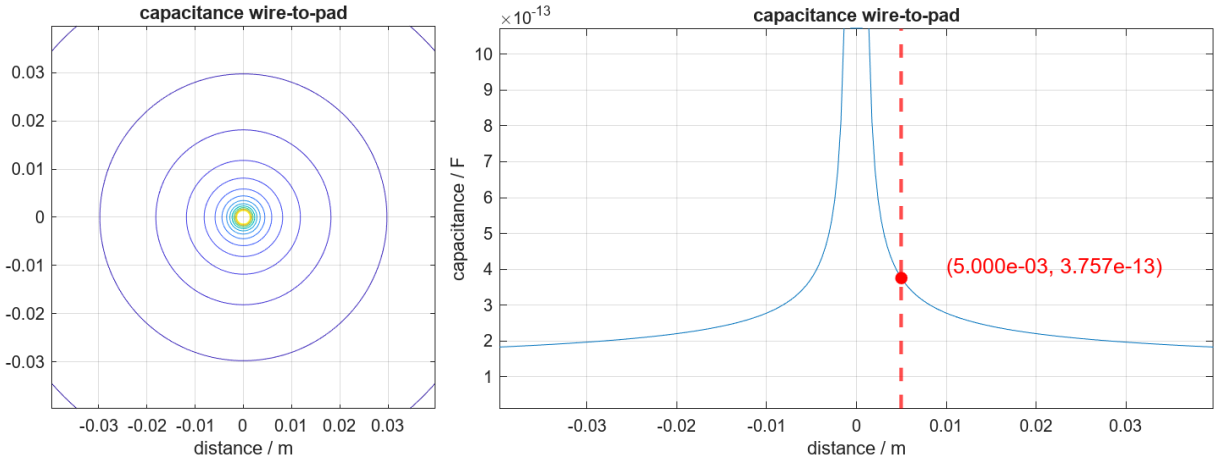

Figure 5: Capacitance wire-to-pad (linear)

To sense the voltage of the electrostatic field a 1 MΩ resistor was used. To make sure that the Impedance does not change, an impedance converter was subsequently introduced. The voltage over the resistor can be calculated the following:

$$\underline{Z_c} = \frac{1}{j\omega C} = \frac{1}{j2\pi f C} = \frac{1}{j \cdot 2\pi \cdot 50\ Hz \cdot 0.37\ pF} = j\underline{\frac{1e12}{37 \cdot \pi}\ \Omega} \tag{3}$$

$$\underline{V_R} = \frac{R}{R + Z_c} \cdot V_{in} = \frac{1\ M\Omega}{1\ M\Omega + Z_c} \cdot 230V = 3.11e-6 + j26.73e-3\ V \tag{4}$$

$$\underline{V_R} = \underline{26.73\ mV\ at\ 89.99°} \tag{5}$$

With this knowledge the needed gain can be calculated. As absolute maximal output 3 V was given:

$$\underline{A_0} = 20 \cdot \log_{10}\left(\frac{V_{in}}{V_R}\right) = 20 \cdot \log_{10}\left(\frac{3V}{V_R}\right) = \underline{41 - j13.65\ dB} \tag{6}$$

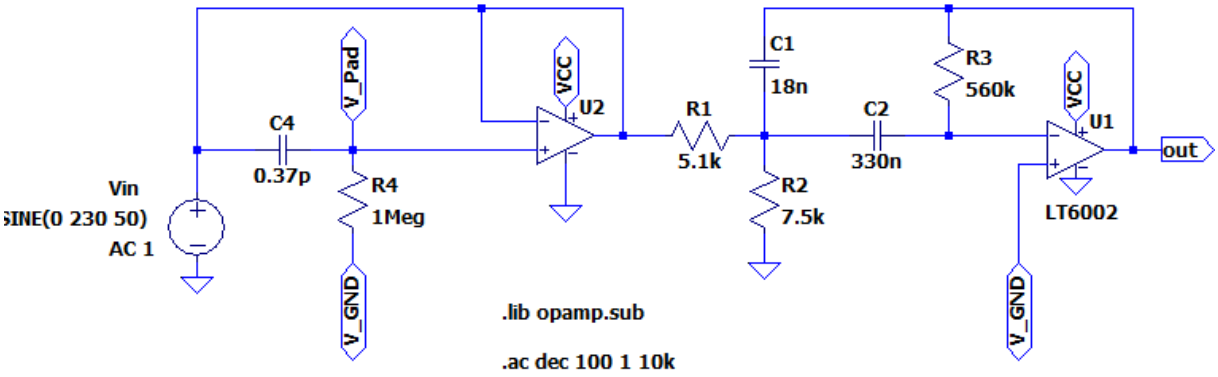

Figure 6: Multi-Feedback-Bandpass-Filter with Gain

With the results a second order Multi-Feedback-Bandpass (MFB) filter was calculated, using the provided idea to use the filter-wizard from AnalogDevices (Analog Devices, 2023). The circuit was then designed and tested in LT-Spice to confirm correct functionality.

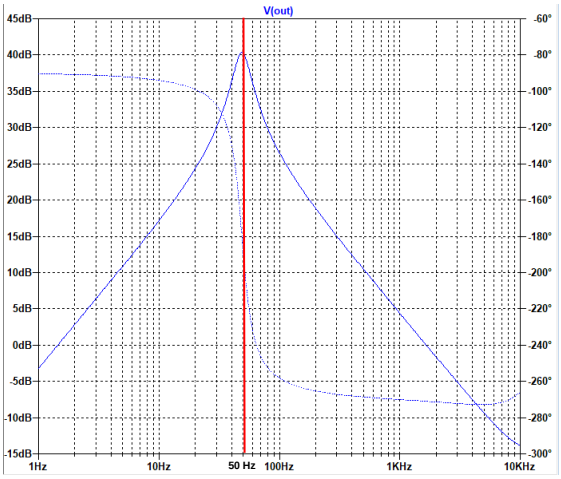

Figure 7: Frequency-Response MFB-Filter

4.3. Electromagnetic field

This section describes how the magnetic field is detected using hall sensors. Using the provided MATLAB script E_B_Field.m (Appendix C), the maximum magnetic field at 5 mm was calculated. The following measurements were conducted at a current of 1 A. The result was a B-Field of 40.08 µVs/m² for a single wire. For double wire a B-Field of 22.41 µVs/m² was measured.

Following that, the theoretical output voltage of the Hall sensor at a 5 mm distance was determined using the provided MATLAB script Uinduced.m (Appendix D). The execution of the script yielded a value of $V_{hall} = 4.72\,mVrms$ (single wire) and $V_{hall} = 2.64\,mVrms$ (double wire). With this information, the required gain can now be computed, considering an absolute maximum output voltage $V_{out} = 3\,V$.

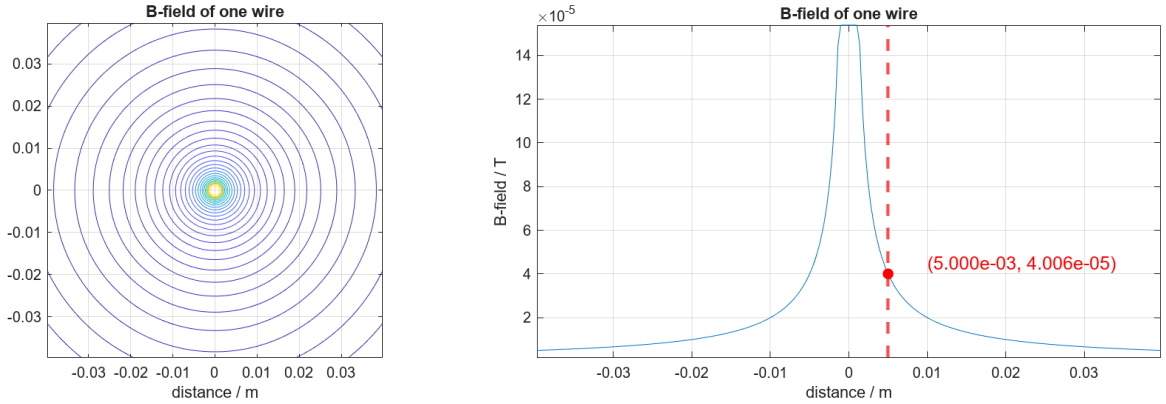

Figure 8: B-Field single wire

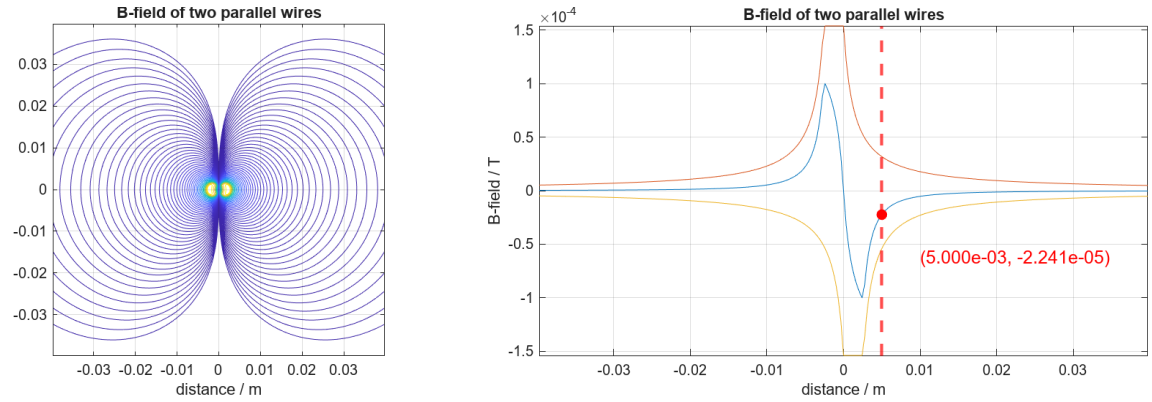

Figure 9: B-Field dual wire

$$\underline{A_0} = 20 \cdot log_{10}\left(\frac{V_{out}}{\sqrt{2} \cdot V_{hall}}\right) = 20 \cdot log_{10}\left(\frac{3\,V}{\sqrt{2} \cdot 4.72\,mV}\right) = \underline{53\,dB} \qquad (7)$$

With the calculated values a filter with the appropriate gain was designed in LT-Spice and the functionality was simulated and tested. Only a simple R-C Filter was used with an amplifier stage. The cut-off frequency was calculated as followed:

$$\underline{fc} = \frac{1}{2\pi \cdot R \cdot C} = \frac{1}{2\pi \cdot 18\,k \cdot 100\,nF} = \underline{88.82\,Hz} \qquad (8)$$

The circuit was finally designed in LT-Spice and simulated with the calculated values.

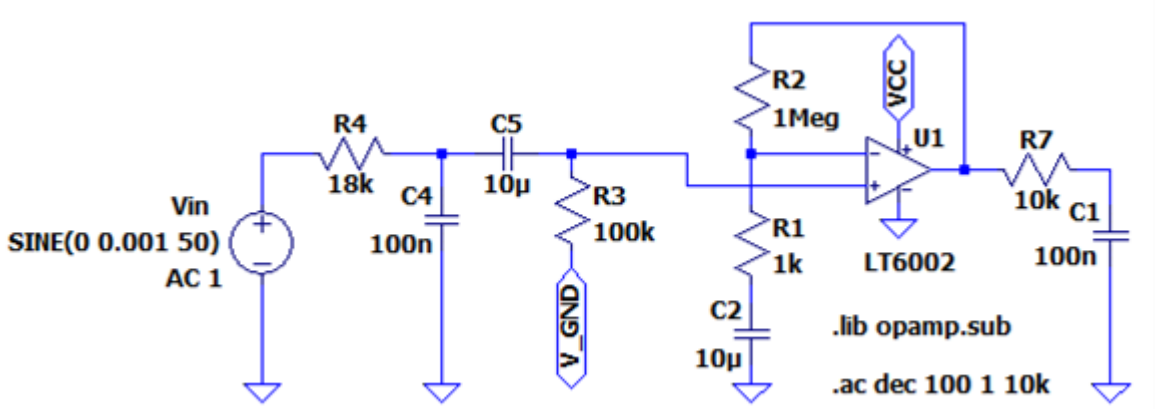

Figure 10: Hall sensor Lowpass with gain

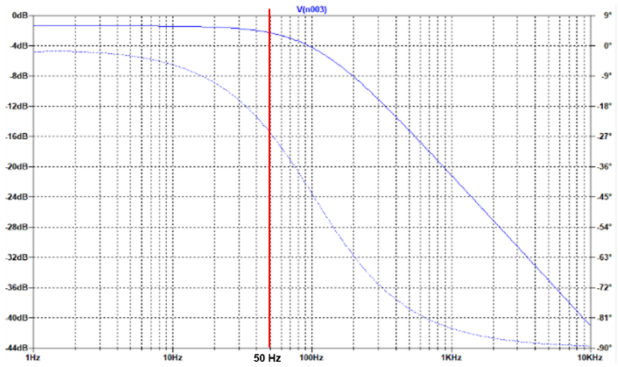

Figure 11: Frequency-Response Hall sensor

5. Implementation

5.1. Power Supply

The power supply is comprised of a Micro-USB Input, delivering 5 V to the board (refer to Figure 12). This voltage traverses the load switch, controlled by the on/off button (see Figure 13). Activation of the on/off button engages the load switch, directing the 5 V signal to a linear DC/DC converter (see Figure 14), which stabilizes the voltage at 3.3 V. This regulated voltage powers both the microcontroller board and cable-monitor board including all the remaining components, as well as all amplifiers and filters. Additionally, larger capacitors decouple all supplies to minimize voltage fluctuations, ensuring precise measurements.

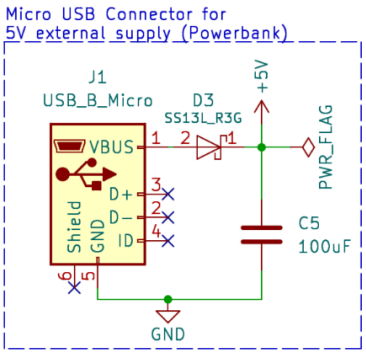

Figure 12: Power Input

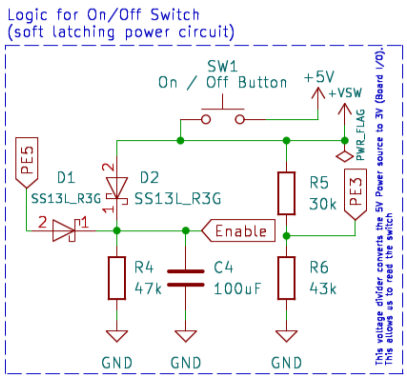

Figure 13: ON/OFF switch

The On/Off circuitry is designed so that once the microcontroller board receives power, it sets pin PE5 high, effectively maintaining its own power supply, a configuration commonly referred to as a soft latching power circuit. Additionally, the state of the switch can be monitored by the microcontroller through pin PE3. This functionality empowers users to define, through software, the power-off sequence for the cable-monitor board and microcontroller. For example, actions such as pressing the off switch for a specific duration or triggering an auto shutdown after a predefined time can be programmed.

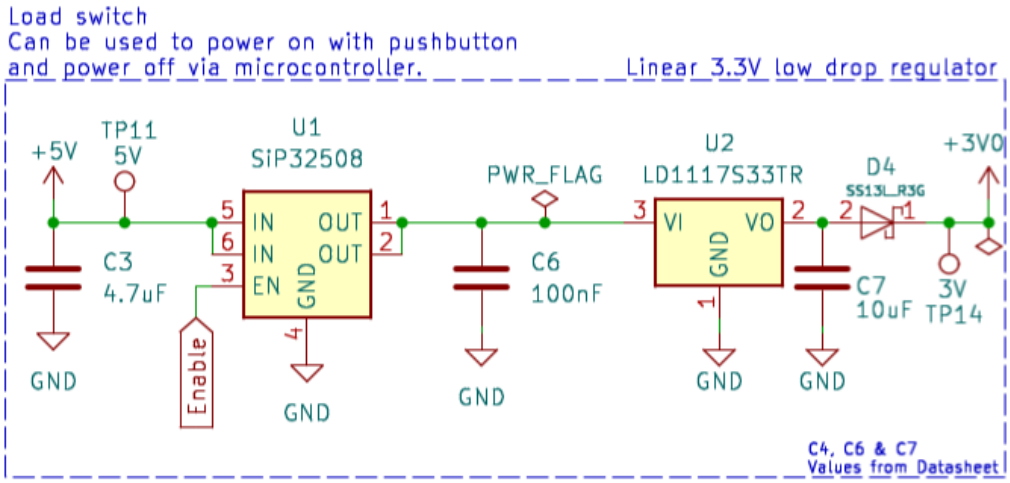

Figure 14: DC/DC converter

5.2. Virtual GND

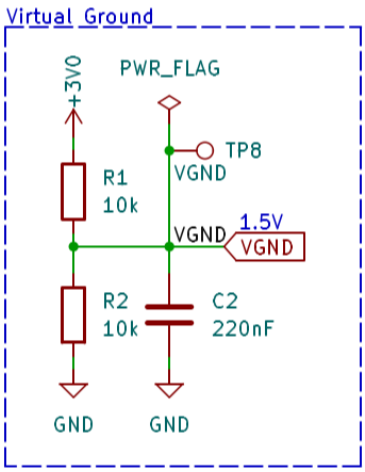

Figure 15: Virtual ground

A virtual ground is formed through a voltage divider, serving the purpose of offsetting the input signals from the sensors (see Figure 15). Furthermore, this virtual ground functions as a reference point in the absence of a signal to sense. As detailed in Chapter 3, Evaluation, the establishment of this new ground is imperative for converting the negative part of the alternating voltage into a positive range, enabling the microcontroller to accurately interpret the signal via its ADC. Additionally, this configuration optimally amplifies the incoming sensor signal in both the positive and negative directions.

5.3. Amplifier and Filter

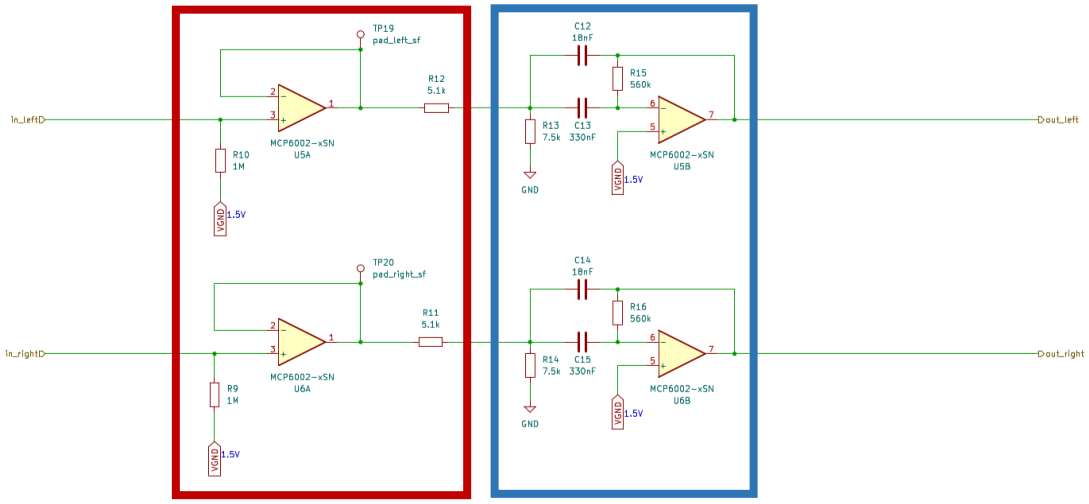

Figure 16: Amplifier and filter for left and right pads (Electrostatic field)

The amplifier and filter serve the purpose of measuring the electrostatic field. Figure 16 illustrates two identical amplifier and filter circuits, each dedicated to either the left or right pad on top of the cable-monitor's PCB. The electrostatic field, converted into a signal by the pad, undergoes the impedance conversion (coloured red) and then passes through the active second-order multi-feedback bandpass (coloured blue).

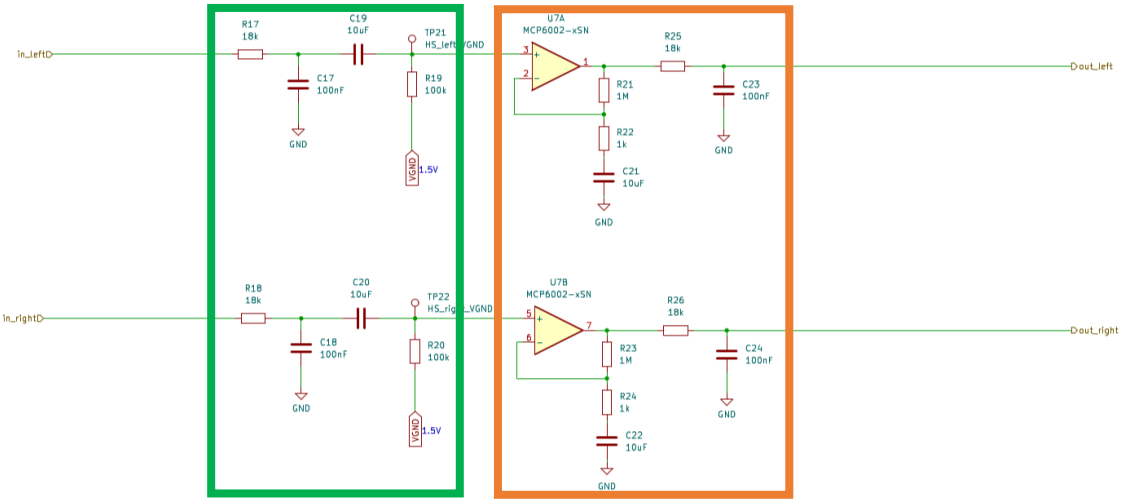

Figure 17: Filter and amplifier for left and right hall sensor (Electromagnetic field)

In this setup, the filter and amplifier work together to measure the electromagnetic field sensed by the hall sensors on top of the cable-monitor's PCB. As depicted in Figure 17, similar to the circuit for the electrostatic measurement (Figure 16), two identical filter and amplifier sets are employed, each dedicated to the left and right hall sensors. Unlike the circuit in Figure 16, there is no need for an impedance converter here. The electromagnetic signal from the hall sensors undergoes processing through a simple R-C low pass filter (coloured green). Subsequently, the signal is amplified with a basic amplifier stage, followed by another R-C low pass filter (coloured orange) to refine the amplified signal.

For more in-depth insights into the evaluation of both filtering and amplifying circuits, refer to Chapter 3. Specifics regarding amplification and cutoff frequency for each circuit can be found in Chapter 4.2 and Chapter 4.3 respectively. The operational amplifier chosen for these circuits and schematics was selected from the template for its compatibility with the design requirements, and its readily availability in ZHAW's inventory. This choice ensures a seamless integration into the project, considering both suitability and practical availability.

5.4. Remaining components

The remaining components include testing points utilized for both measurement and calibration of the cable-monitor board, decoupling capacitors, the interface connecting the microcontroller and the cable-monitor board, and optional features such as the buzzer, discussed in detail in Chapter 4.1.3. Through the interface, critical signals like the processed electromagnetic and electrostatic field signals reach the microcontroller's ADC, alongside various I/O vias and the supply voltage for the microcontroller board. For a comprehensive view, refer to the complete schematic in Appendix A for further details.

5.5. PCB Layout

Some of the most crucial considerations in PCB layout include the GND plane, the placement of hall sensors and pads, and the size of the pads.

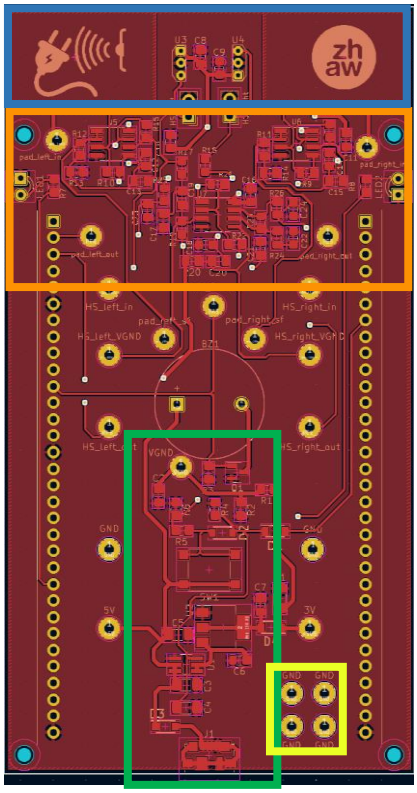

Figure 18: PCB top layer with GND plane

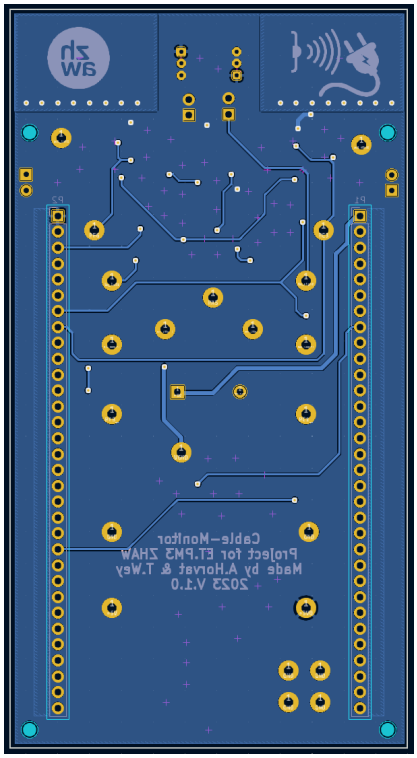

Figure 19: PCB bottom layer with 3 V plane

Equally important are aspects that significantly contribute to the overall design, such as the testability of the board. The inclusion of testing points on key signals enables the verification of the PCB's correct operation.

In Figure 18, the red area on top of the board represents the GND plane. This GND plane serves to enhance signal integrity, minimize electrical noise, reduce voltage drop, and provide substantial protection against electrostatic discharge (ESD) and electromagnetic interference (EMI). Similarly, the bottom layer is complemented with a 3 V power plane (see Figure 19), further enhancing protection against EMI and improving power distribution, consequently minimizing voltage drop and improving signal integrity.

Separating the layout in functional blocks helps to keep an organised overview of the layout as well as having positive effects on signal integrity.

The orange-coloured block represents the filtering and amplifying circuits explained in Chapter 5.3. Separating the signal traces within this block helps reduce interference from other traces.

The pads and hall sensors are positioned at the front of the PCB to optimize the measurement of the electromagnetic and electrostatic fields (blue-coloured block). Additionally, the pads have been maximized in size to accurately determine the position of the fields.

For calibration purposes, the person holding the cable-monitor must touch GND. To facilitate this, four testing points have been placed closely together, allowing the person holding the board to place a finger on them (yellow-coloured block).

Finally, all power-related components and lines have been placed close together to minimize electromagnetic interference and reduce impedance (green-coloured block).

6. Testing

The following measurements and tests were conducted under average laboratory conditions using the following measuring devices:

- Tektronix TDS 2012C Two Channel Digital Storage Oscilloscope
- Agilent Technologies U3402A Dual Display Multimeter
- TTi TG5011 50 MHz Function/Arbitrary/Pulse Generator

Table 1 testing table

Test item, Description	**Test conditions**	**Expected, Tolerance**	**Measured result**	**Comparison, verdict**	**Remarks, Discussion**
Power supply voltage at TP11 (5V)	Powered with external powerbank connected to Micro-USB input. No input signal	5 VDC - Diode forward voltage = **4.7 VDC** ± 200 mV	4.66 VDC	deviation - 40 mV passed	passed
DC/DC Converter output at TP14 (3V)	No input signal	3.3 VDC – Diode forward voltage = **3.0 VDC** ± 100 mV	2.99 VDC	deviation -10 mV passed	passed
DC Operating point (Virtual GND)	3 VDC at TP14, no input signal	1.5 VDC ± 20 mV	1.48 VDC	deviation -20 mV passed	passed
Gain pad measurement at TP12	Input signal at TP9: 50 mVpp 50 Hz sine	3 Vpp ± 200 mV gain: 40 dB ± 2% (from simulation)	2.48 Vpp Gain: 34 dB	deviation Voltage: 520 mV Gain: 15 %	Failed, deviation too high
Gain hall sensor measurement at TP17	Input signal at TP15: 5 mVpp 50 Hz sine	2.8 Vpp ± 200 mV gain: 55 dB ± 2% (from simulation)	2.54 Vpp Gain 53.8 dB	deviation Voltage: 260 mV Gain: 2.2%	Failed, deviation too high

The measurements on the pad and hall sensor exceeded the deviations, potentially attributed to imprecise resistor and capacitor values and the supply voltage not being perfectly stable. Nevertheless, the processed signals arrive at the microcontroller inputs cleanly, exhibiting minimal noise, making them perfectly usable. Further data processing can be accomplished through software to compensate any further deviations. For detailed visualizations of the pad and hall sensor measurements, please refer to Figures 20 and 21, which display the signals measured by the oscilloscope.

Additional measurements conducted with the predefined measurement setup provided by ZHAW are available in Appendix E.

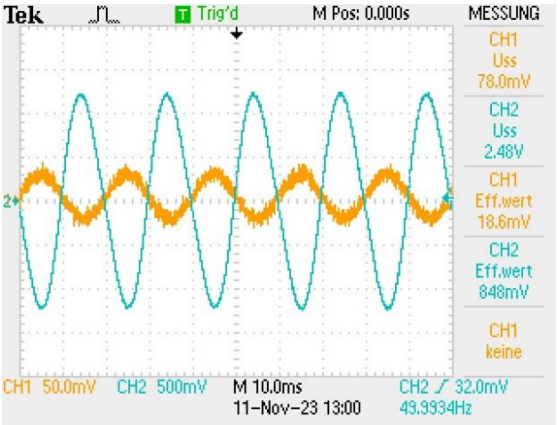

Figure 20: Pad gain measurement

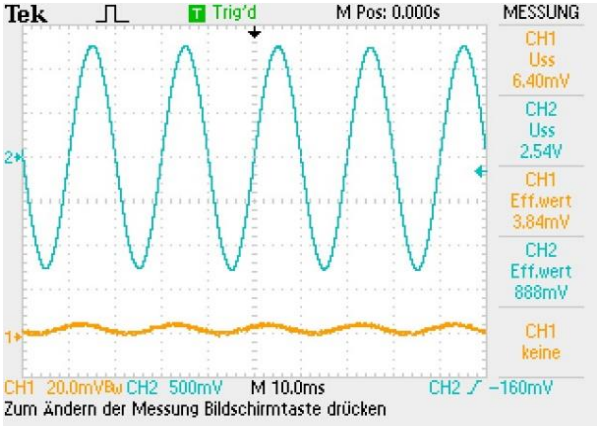

Figure 21: Hall sensor gain measurement

7. Project Management

To enhance the clarity of the project overview, we developed a Gantt Diagram, as outlined in Appendix E. This visualization allowed us to efficiently allocate various tasks from the timeline, offering a comprehensive and easily digestible summary of the project milestones and responsibilities.

- Sensor Board Design:
  - Simulation and Calculation (MATLAB): Assigned to Timo.
  - Schematic drawing and PCB design: Assigned to Alejandro.
  - Research and component gathering: Both Timo and Alejandro worked together on this.
- PCB Board:
  - Soldering and testing: Both Timo and Alejandro contributed to soldering the PCBs and conducted testing and demonstrations.
- Firmware:
  - Code analysis: Both team members participated.
  - Touch Interface code writing: Assigned to Timo.
  - Signal sensing code writing: Assigned to Alejandro.
  - Testing and demonstration: Both Timo and Alejandro participated in testing the firmware and demonstrating its functionality.
- Documentation:
  - HW-Report, FW-Documentation, and Presentation: Done continuously as a team effort.

8. Conclusion

When planning, we carefully worked out the hardware details, making it easy to implement documents like the schematic. We used MATLAB files for calculations, making it simple to adjust values and explore different options. Assembling the print was smooth, thanks to our experience. The print worked well from the start, with only minor adjustments needed for resistor values due to high pad gain deviations. After tweaking, it worked perfectly. To improve noise reduction in the future, we could consider using larger decoupling capacitors and adding guard rings on the PCB.

9. List of references

Analog Devices. (2023). *Analog Filter Wizard*. Von https://tools.analog.com/en/filterwizard/ abgerufen

Hochreutener, H. (2023). Cable_Monitor.docx. ZHAW. Retrieved from \\shared.zhaw.ch\pools\t\T-ISC-ET-PM3 (not publicly available)

10. Figure list

11. Appendix

A - Schematics

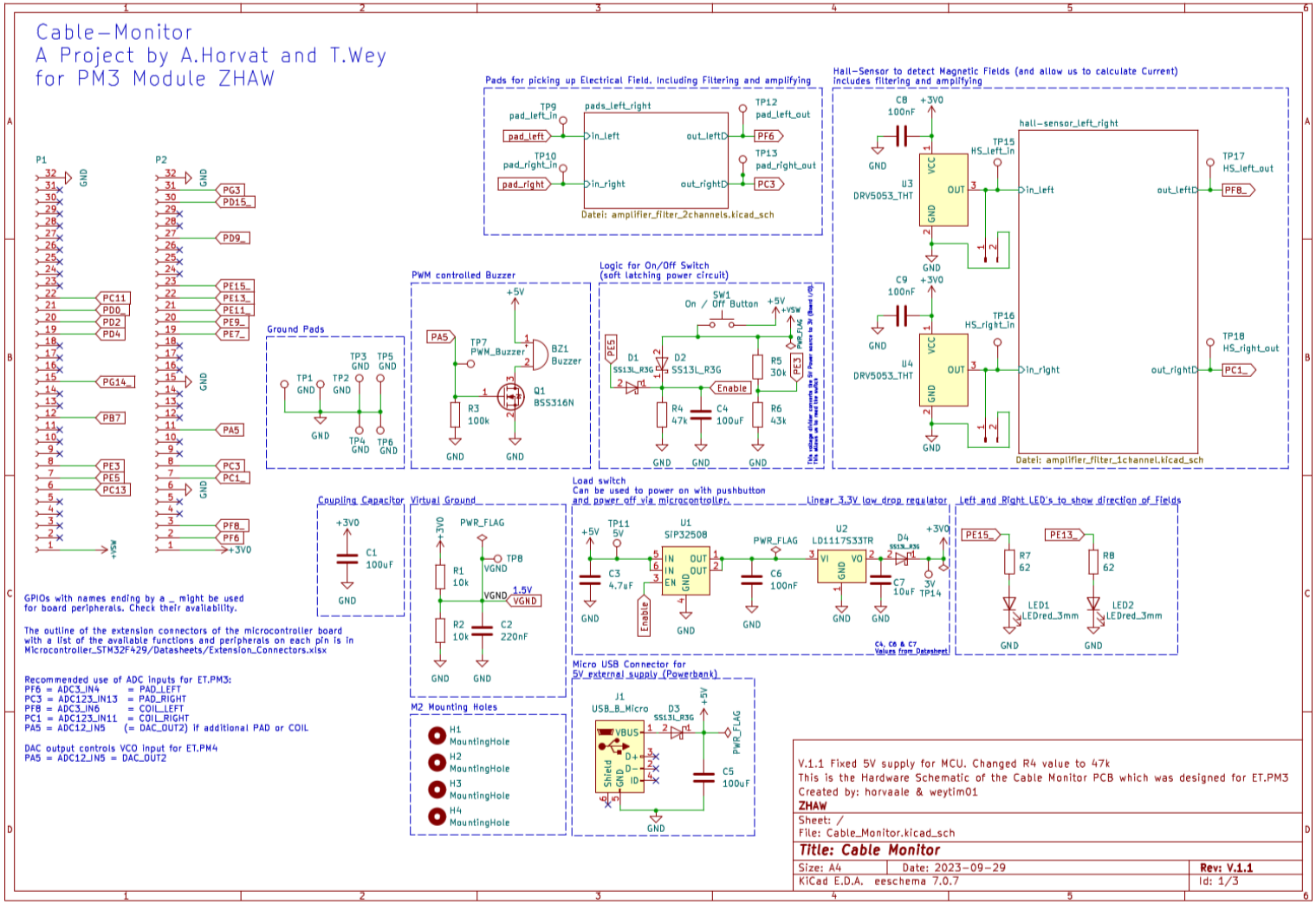

Figure 22: Main schematic

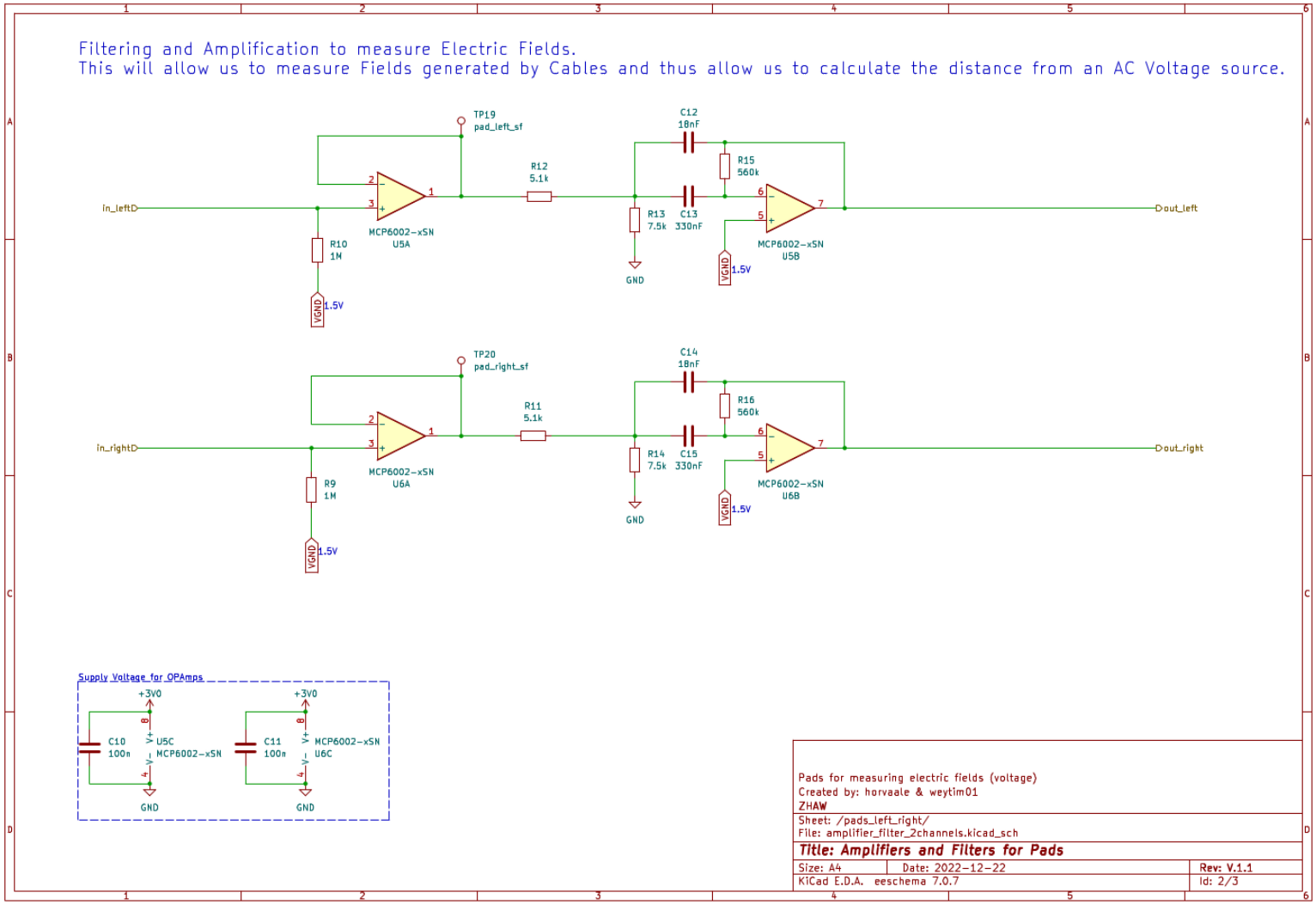

Figure 23: Pad amplification and filtering schematic

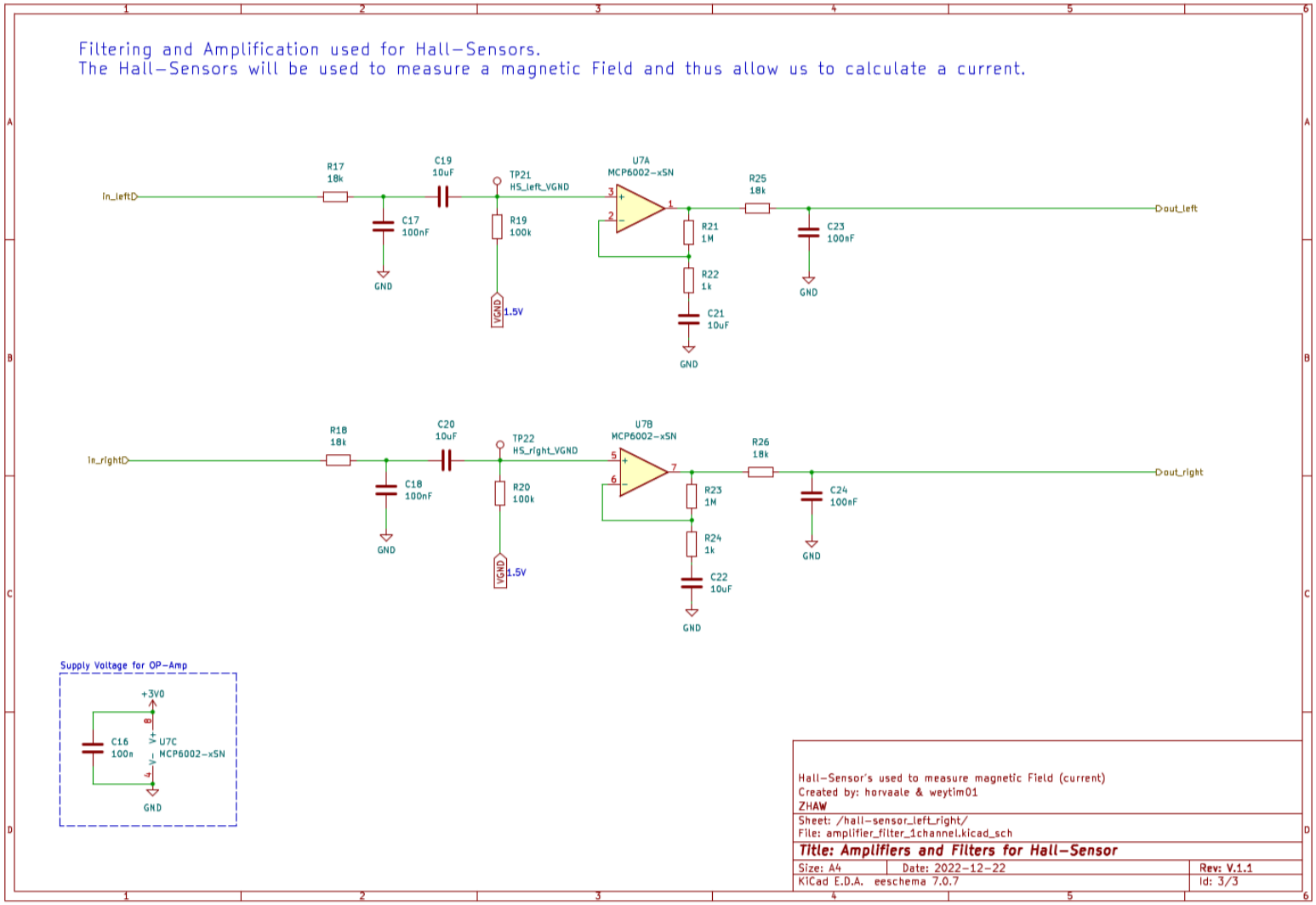

Figure 24: Hall sensor amplification and filtering schematic

B - PCB

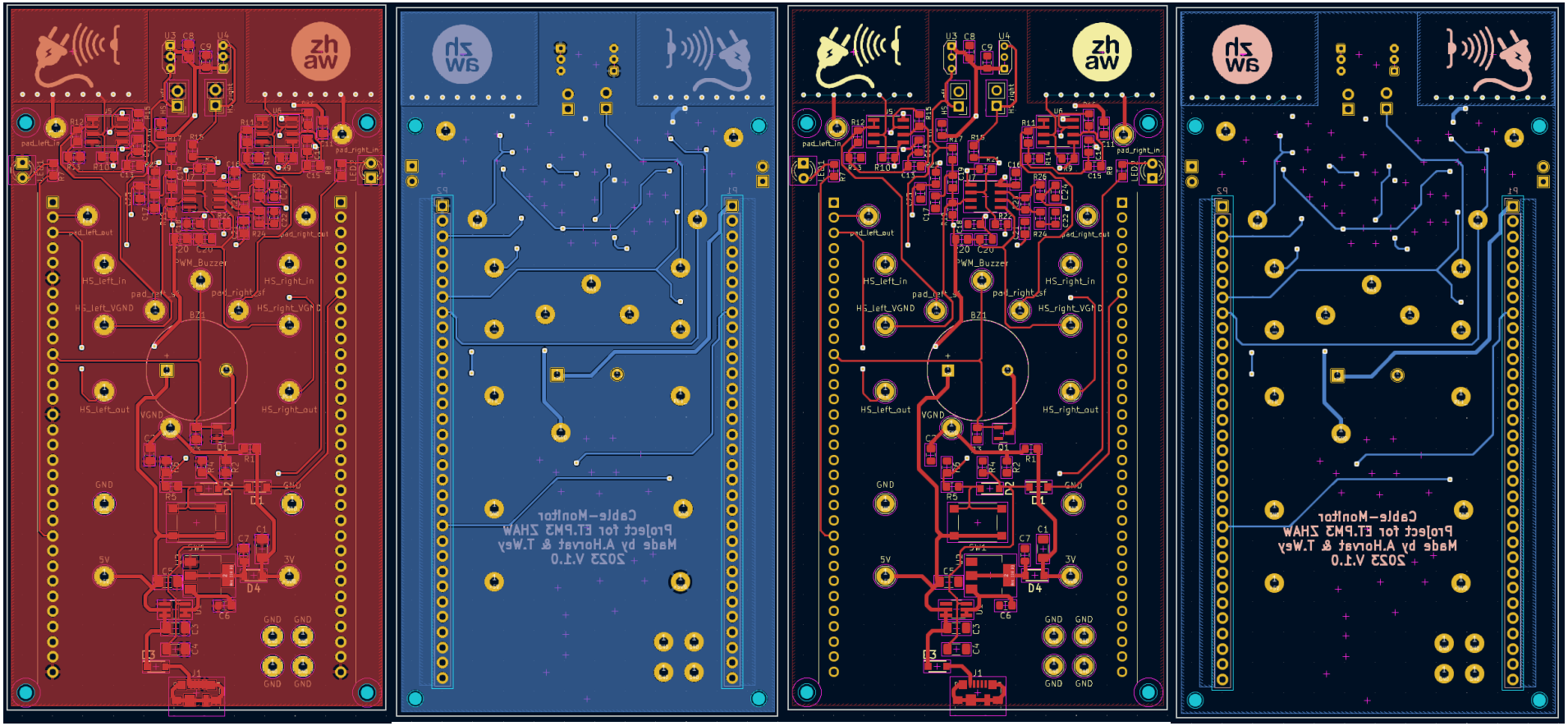

Figure 25: From left to right: top layer with GND plane, bottom layer with 3 V plane, top layer without GND plane, bottom layer without 3 V plane.

C - E-B_Field.m

```
%% Calculate the E- and B-fields of a mains cable
% Voltage set to 230V
% Current normalised to 1A
% (c) hhrt@zhaw.ch 06.02.2020
clc; clear; close all;
format compact; format short eng;
set(groot,'defaultAxesXGrid','on')
set(groot,'defaultAxesYGrid','on')

%% Geometry             % All dimensions in m or m2
length_pad = 15.62e-3;
with_pad = 22.86e-3;
A_wire = 1.5e-6;         % Conductor cross-section in m2
d_wires = 2.6e-3;        % Outer diameter of isolated conductor = distance of wire↙
centers
d_pad = sqrt(2*length_pad*with_pad);  % Length of pad which picks up the electric↙
field of the wire
%% Pre-calculation
r_wire = sqrt(A_wire/pi);        % Radius of the wire
N = 115; inc = r_wire/2;         % Grid dimension and grid spacing in mm
[X,Y] = meshgrid(inc*(-N:1:N), inc*(-N:1:N));
scrsz   = get(0,'ScreenSize');
figure('name', 'Capacity to earth and H-field of one wire and of two wires',↙
'Position',[10,10,scrsz(3)-20,scrsz(4)-100])

%% Calculate capacity of pad to wire
%  Approach: Calculate capacity with formula for parallel wires
%  As with capacitors in series the smaller value is dominant, the
%  length of the pad and the radius of the wire are taken for calculation.
%  The capacitance value is thus a bit underestimated.
distance = sqrt(X.^2+Y.^2);
C = 8.85e-12*pi*d_pad ./ log(distance/r_wire);
Cmax = 8.85e-12*pi*d_pad / log(2);  % Limit when wire and pad touch
C(1+N-2:1+N+2,1+N-2:1+N+2) = Cmax;

subplot(331);
v = Cmax*logspace(-3,0);
contour(X,Y,C,v); axis equal;
grid;
title('capacitance wire-to-pad');
xlabel('distance / m');

%=========================================================================
subplot(332);
hold on;
xline(0.005, 'r--', 'LineWidth', 2);
plot(X(1+N,:), C(1+N,:));
title('capacitance wire-to-pad');
ylabel('capacitance / F');
xlabel('distance / m');
axis([-N*inc, N*inc, Cmax/100, Cmax]);
% Add coordinates at the intersection point
xlineIntersection = 0.005;
% Interpolate y-value at intersection
ylineIntersection = interp1(X(1+N,:), C(1+N,:), xlineIntersection);
% Add a filled red dot at the intersection
scatter(xlineIntersection, ylineIntersection, 50, 'r', 'filled');
text(xlineIntersection+0.005, ylineIntersection, sprintf('(%.3e, %.3e)', ...
    xlineIntersection, ylineIntersection), 'Color', 'red', 'FontSize', 12, ...
    'VerticalAlignment', 'bottom');
box on;
hold off;
subplot(333);
semilogy(X(1+N,:), abs(C(1+N,:)));
title('capacitance wire-to-pad');
ylabel('capacitance / F'); xlabel('distance / m');
axis([-N*inc, N*inc, Cmax/100, Cmax]);
%=========================================================================
%% Calculate B-field of one wire
u = 1.257e-6;
R = sqrt(X.*X + Y.*Y);
B = u./(2*pi*R);
Bmax = u./(2*pi*d_wires/2);    % Limit when wire touched
B = min(B, Bmax);        % B-field would decrease in the the wire

subplot(334);
v = Bmax*logspace(-3,0);
contour(X,Y,B,v); axis equal;
title('B-field of one wire');
xlabel('distance / m');
grid;
subplot(335);
hold on;
plot(X(1+N,:), B(1+N,:));
xline(0.005, 'r--', 'LineWidth', 2);
title('B-field of one wire');
ylabel('B-field / T'); xlabel('distance / m');
axis([-N*inc, N*inc, Bmax/100, Bmax]);
% Add coordinates at the intersection point
% Interpolate y-value at intersection
ylineIntersection = interp1(X(1+N,:), B(1+N,:), xlineIntersection);
% Add a filled red dot at the intersection
scatter(xlineIntersection, ylineIntersection, 50, 'r', 'filled');
text(xlineIntersection+0.005, ylineIntersection, sprintf('(%.3e, %.3e)', ...
    xlineIntersection, ylineIntersection), 'Color', 'red', 'FontSize', 12, ...
    'VerticalAlignment', 'bottom');
box on;
hold off;
subplot(336);
semilogy(X(1+N,:), abs(B(1+N,:)));
title('B-field of one wire');
  ylabel('|B-field| / T'); xlabel('distance / m');
axis([-N*inc, N*inc, Bmax/100, Bmax]);

%% Calculate resulting B-field of two parallel wires in same cable
R1 = sqrt((X+d_wires/2).*(X+d_wires/2) + Y.*Y);
B1 = u./(2*pi*R1);
B1 = min(B1, Bmax);         % B-field would decrease in the the wire
R2 = sqrt((X-d_wires/2).*(X-d_wires/2) + Y.*Y);
B2 = -u./(2*pi*R2);    % Current in oposite direction
```

```
B2 = max(B2, -Bmax);        % B-field would be 0 in the center of the wire
B12 = B1 + B2;
subplot(337);
v = Bmax*logspace(-3,0);
contour(X,Y,abs(B12),v);
axis equal;
title('B-field of two parallel wires');
xlabel('distance / m');
grid;
subplot(338);
plot(X(1+N,:), B12(1+N,:), X(1+N,:), B1(1+N,:), X(1+N,:), B2(1+N,:));
hold on;
xline(0.005, 'r--', 'LineWidth', 2);

title('B-field of two parallel wires');
ylabel('B-field / T'); xlabel('distance / m');
axis([-N*inc, N*inc, -Bmax, Bmax]);
% Add coordinates at the intersection point
% Interpolate y-value at intersection
ylineIntersection = interp1(X(1+N,:), B12(1+N,:), xlineIntersection);
% Add a filled red dot at the intersection
scatter(xlineIntersection, ylineIntersection, 50, 'r', 'filled');
text(xlineIntersection+0.005, ylineIntersection-0.5e-4, sprintf('(%.3e, %.3e)', ...
    xlineIntersection, ylineIntersection), 'Color', 'red', 'FontSize', 12, ...
    'VerticalAlignment', 'bottom');
hold off;

subplot(339);
semilogy(X(1+N,:), abs(B12(1+N,:)));
title('B-field of two parallel wires');
  ylabel('|B-field| / T'); xlabel('distance / m');
axis([-N*inc, N*inc, Bmax/100, Bmax]);
```

D - Uinduced.m

```
%% Calculate the induced voltage of a magnetic field
%  into an inductor coil with ferrite core
%  Rough estimation for an *unshielded* inductor
%  (c) hhrt@zhaw.ch 13.02.2020
clc; clear; close all;
format compact; format short eng;
% Known values
B0 = 2.241e-5;              % Magnetic field in air (from simulation)
f = 50;                     % Frequency of mains
d = 5e-3;                   % Diameter of coil (datasheet)
l = 3e-3;                   % Length of coil (datasheet)
L = 10e-3;                  % Inductance of coil (datasheet)
ur = 300;                   % Relative permeability of ferrite (estimation)
% Calculation
u0 = 1.257e-6;              % Permeability of vacuum
A = pi*(d/2)^2;             % Cross section of coil
Br = B0*ur;                 % Field in the ferrite body is stronger than in air
N = sqrt(L*l/(u0*ur*A)) % Number of turns of the coil
% The above formula is only correct for long air coils.
% It should be fine as an rough approximation.
% Check if the calculated N is plausible.
% Result
U = N*2*pi*f*A*Br       % Induced voltage in the coil
```

E – Gantt-Diagram

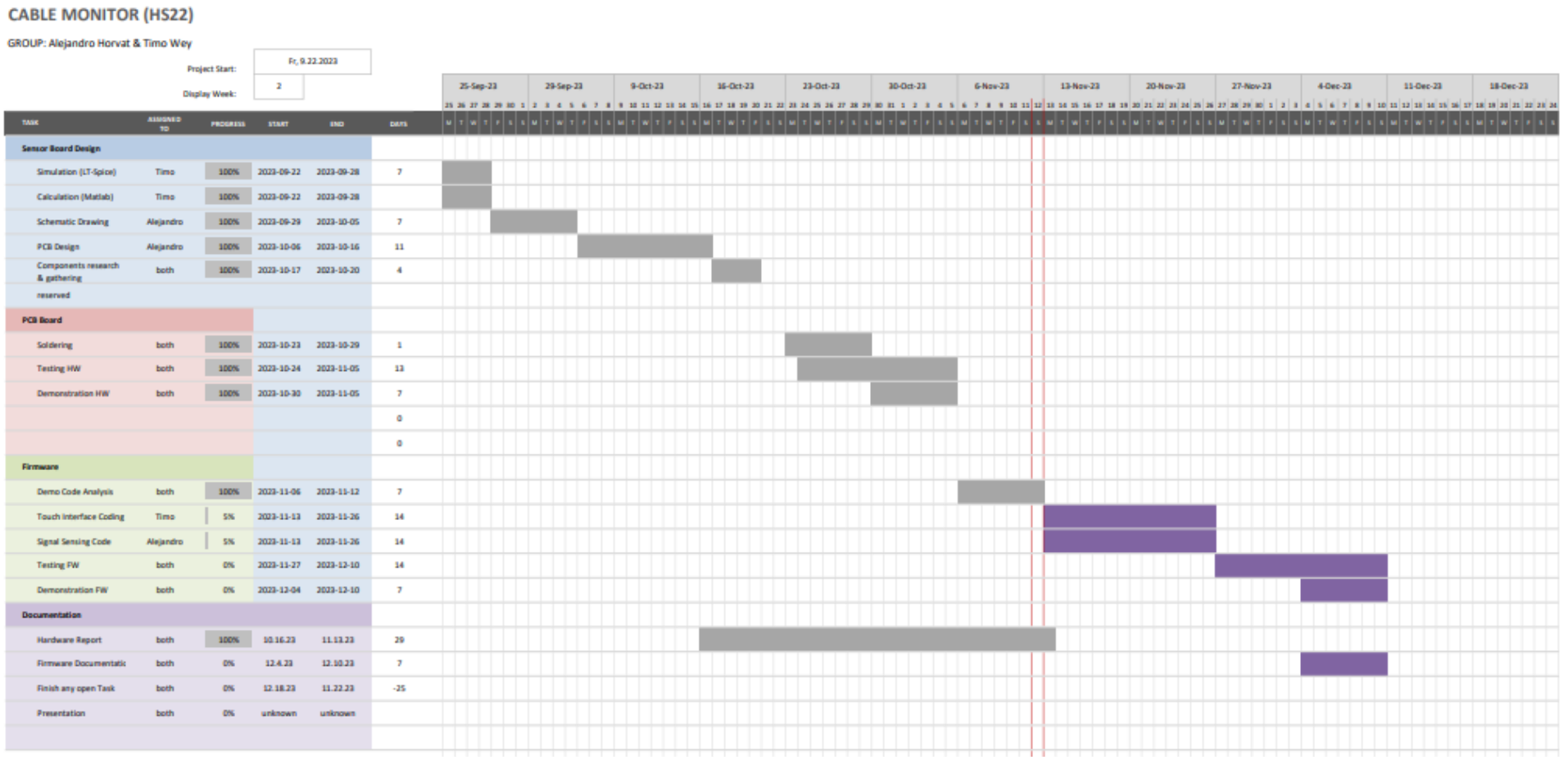

TASK	ASSIGNED TO	PROGRESS	START	END	DAYS
Sensor Board Design					
Simulation (LT-Spice)	Timo	100%	2023-09-22	2023-09-28	7
Calculation (Matlab)	Timo	100%	2023-09-22	2023-09-28	
Schematic Drawing	Alejandro	100%	2023-09-29	2023-10-05	7
PCB Design	Alejandro	100%	2023-10-06	2023-10-16	11
Components research & gathering	both	100%	2023-10-17	2023-10-20	4
reserved					
PCB Board					
Soldering	both	100%	2023-10-23	2023-10-29	1
Testing HW	both	100%	2023-10-24	2023-11-05	13
Demonstration HW	both	100%	2023-10-30	2023-11-05	7
					0
					0
Firmware					
Demo Code Analysis	both	100%	2023-11-06	2023-11-12	7
Touch Interface Coding	Timo	5%	2023-11-13	2023-11-26	14
Signal Sensing Code	Alejandro	5%	2023-11-13	2023-11-26	14
Testing FW	both	0%	2023-11-27	2023-12-10	14
Demonstration FW	both	0%	2023-12-04	2023-12-10	7
Documentation					
Hardware Report	both	100%	10.16.23	11.13.23	29
Firmware Documentatic	both	0%	12.4.23	12.10.23	7
Finish any open Task	both	0%	12.18.23	11.22.23	-25
Presentation	both	0%	unknown	unknown	

E – Measurements

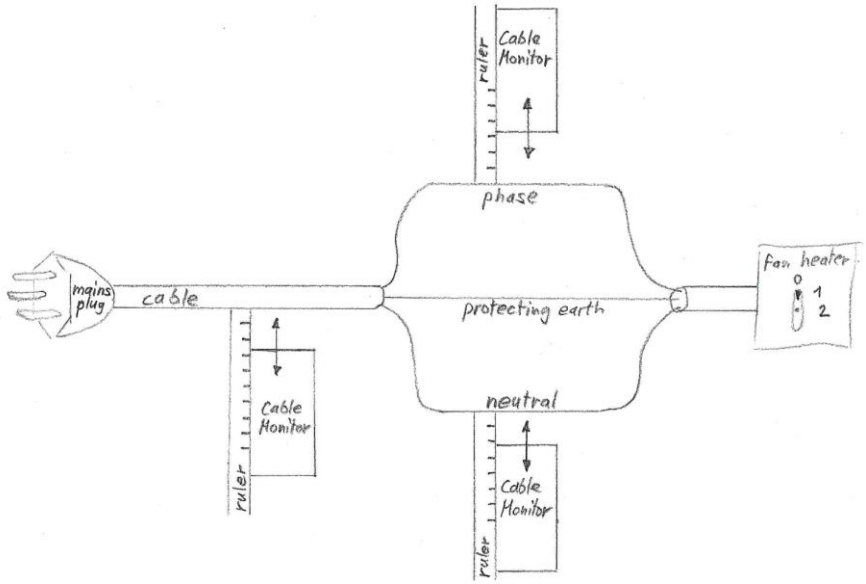

Figure 26: measurement setup drawing from ZHAW

(Hochreutener, 2023)

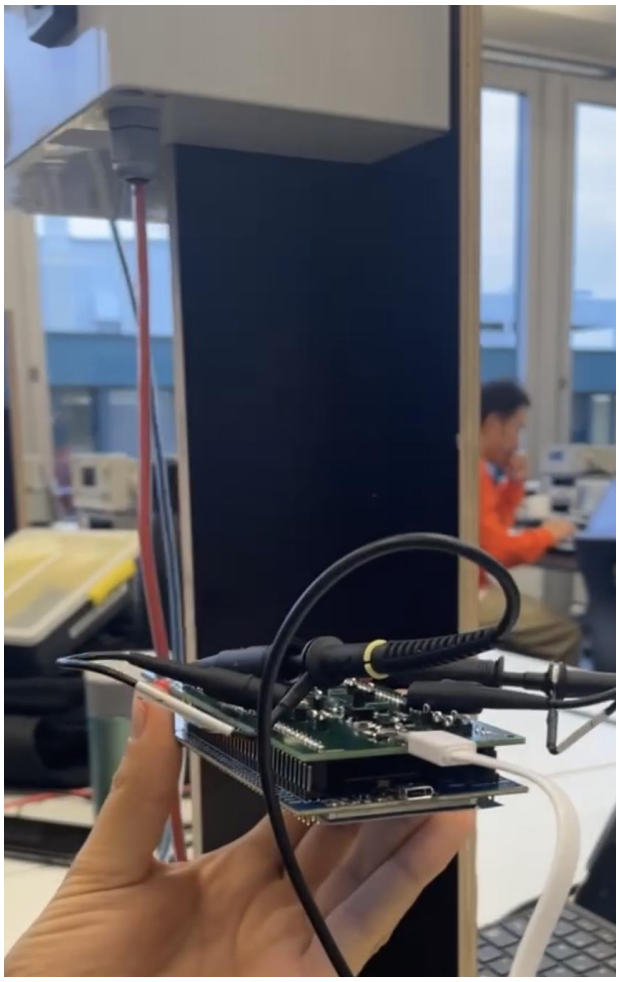

Figure 27: Measurement setup from ZHAW, with live cable and adjustable current

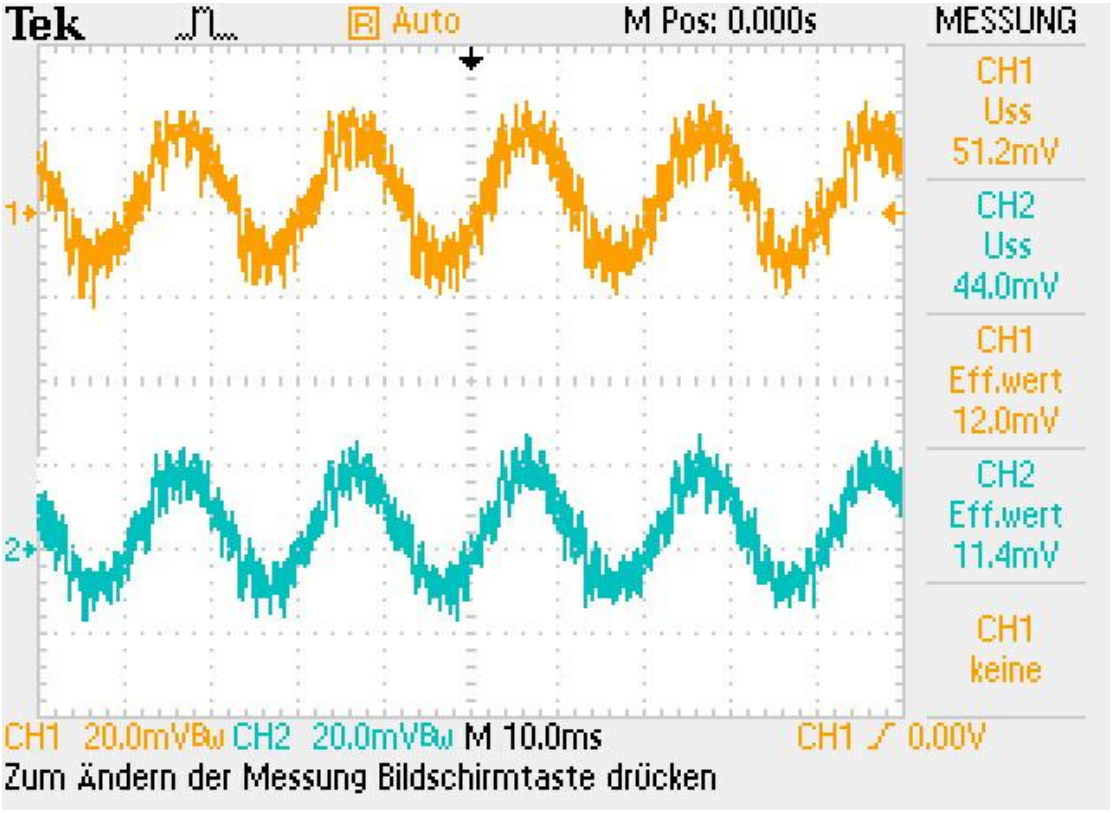

Figure 28: Pad input 1.2 A at 10mm

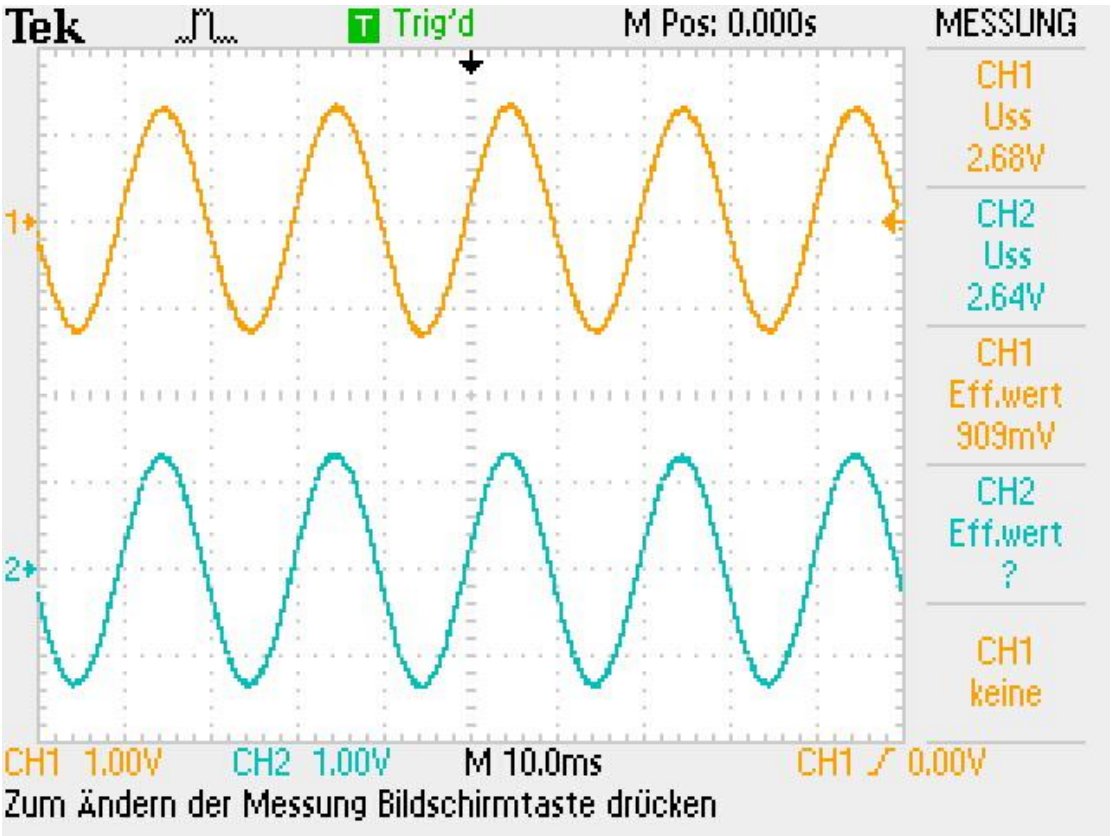

Figure 29: Pad output 1.2 A at 10mm

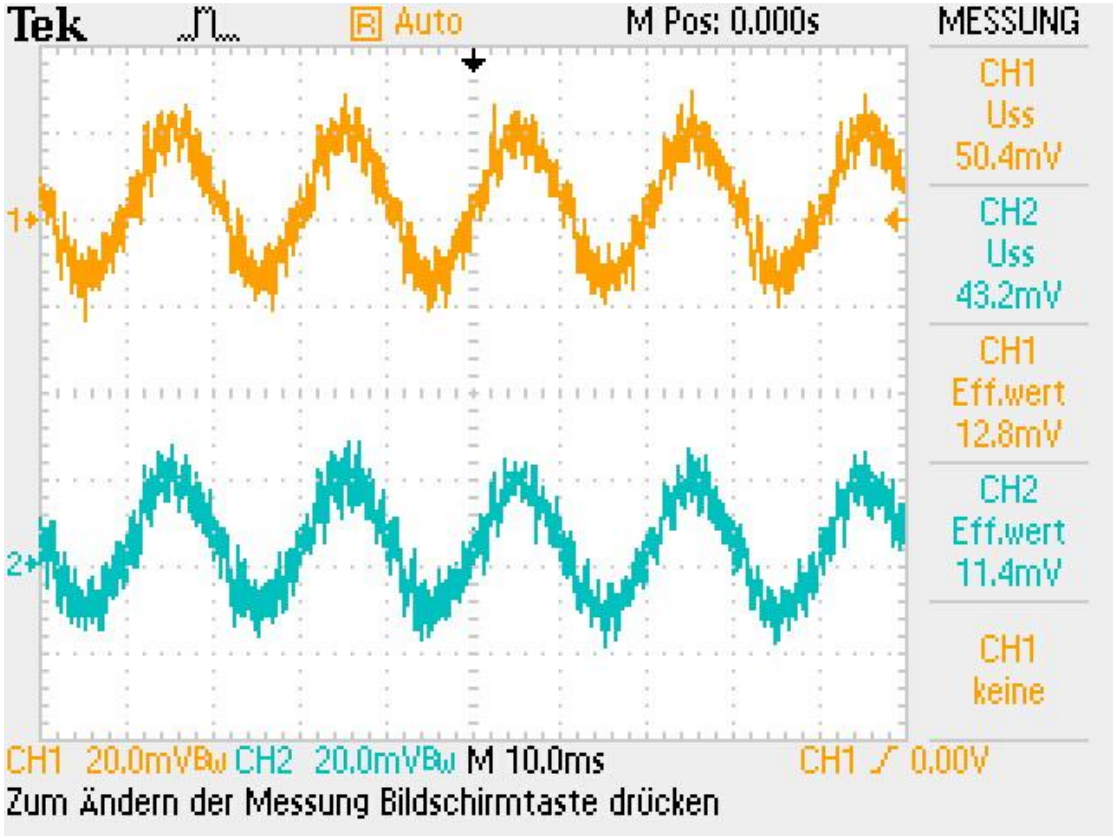

Figure 30: Pad input 5 A at 10mm

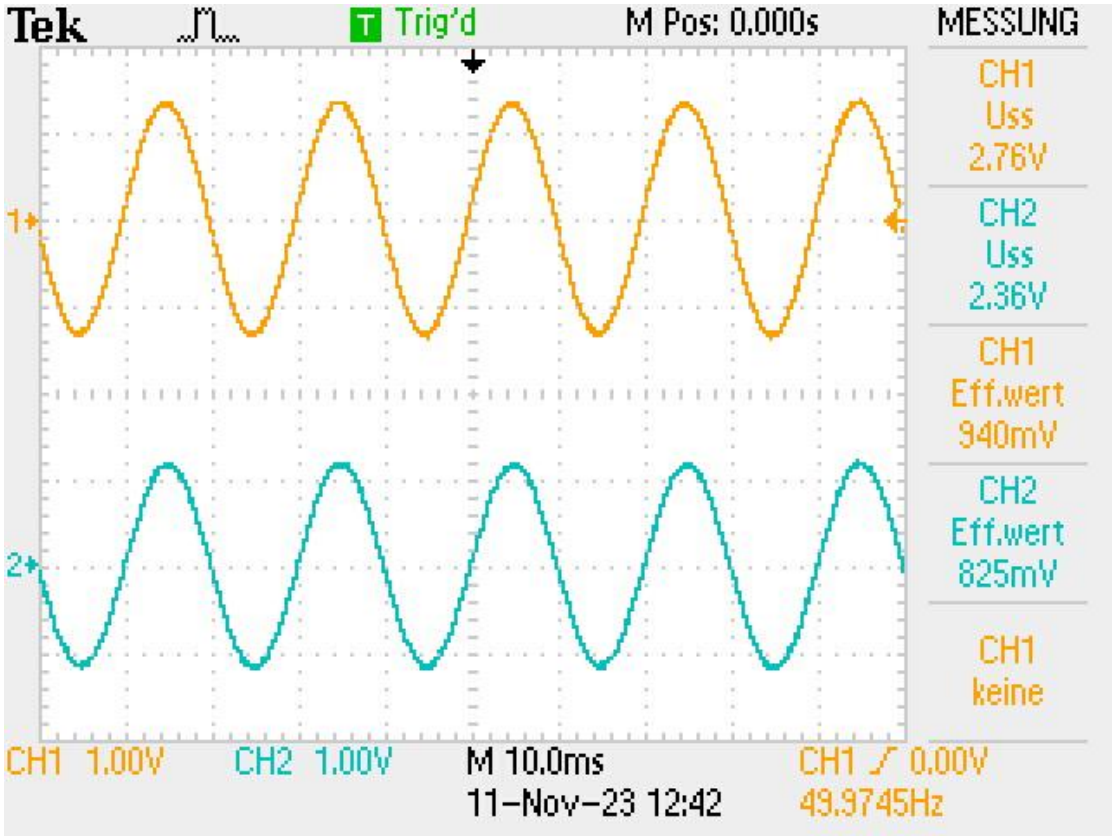

Figure 31: Pad output 5 A at 10mm

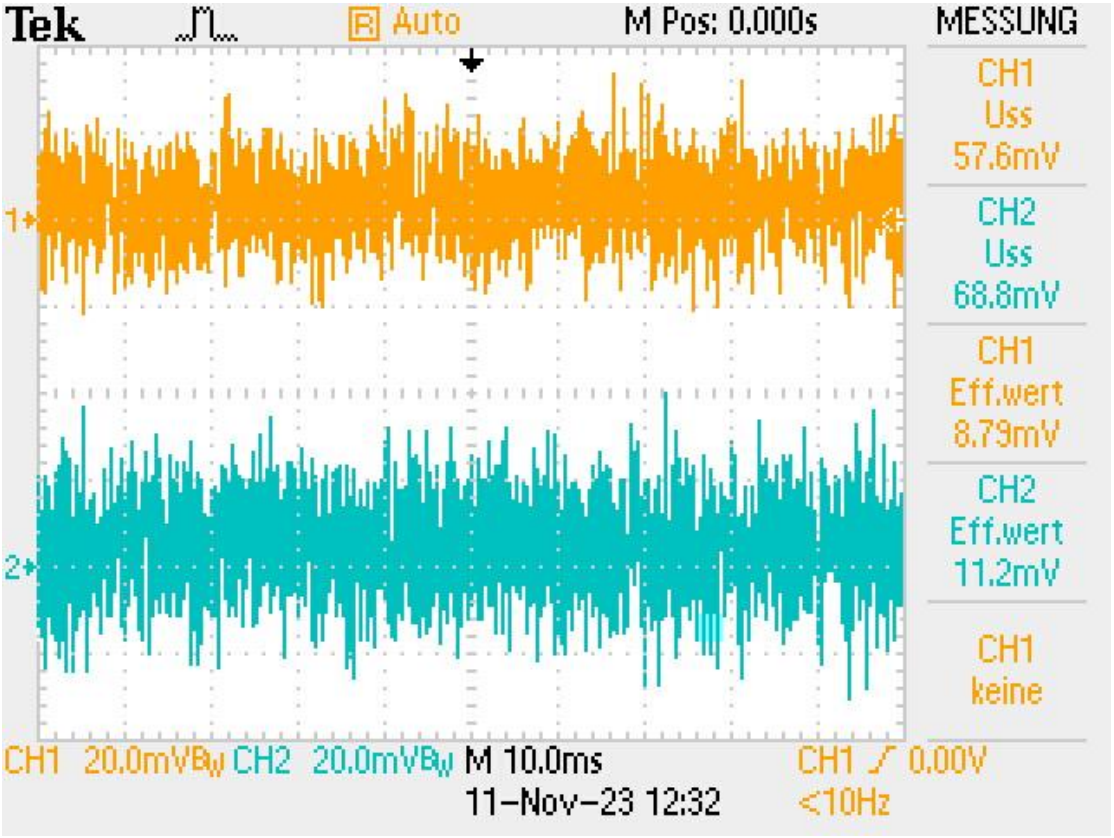

Figure 32: Hall sensor input 1.2 A at 10mm

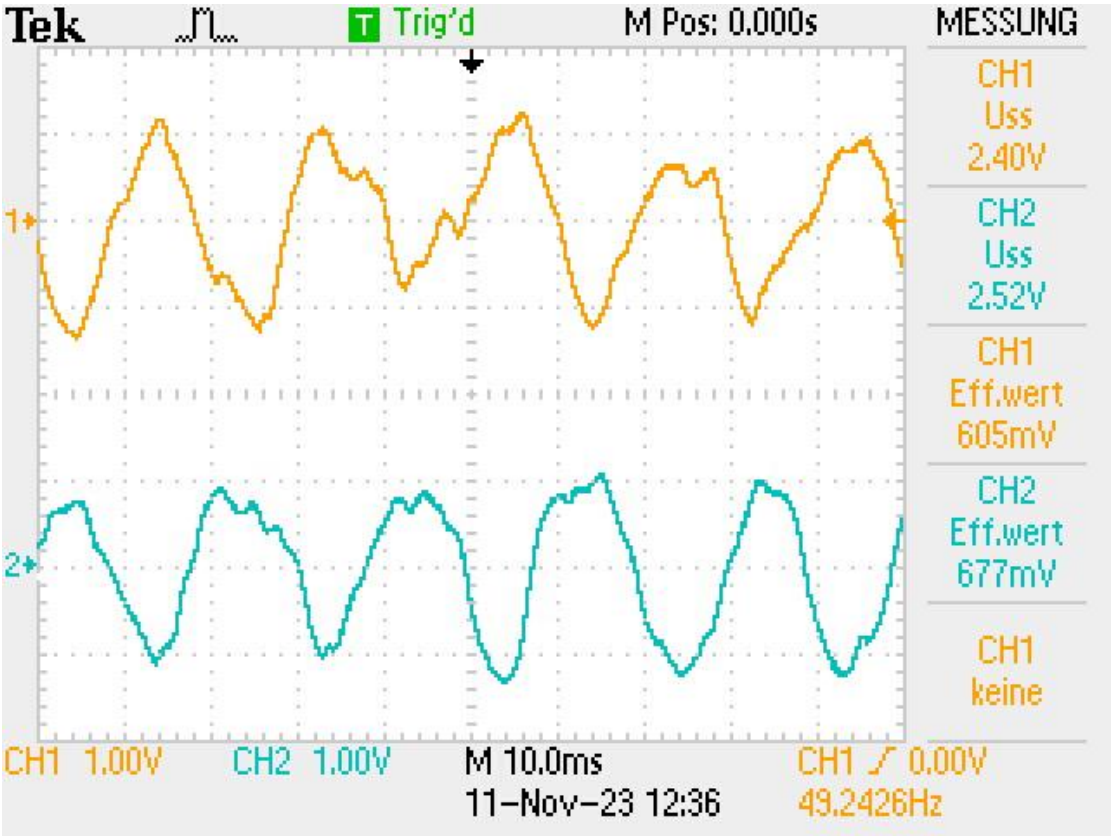

Figure 33: Hall sensor output 1.2 A at 10 mm

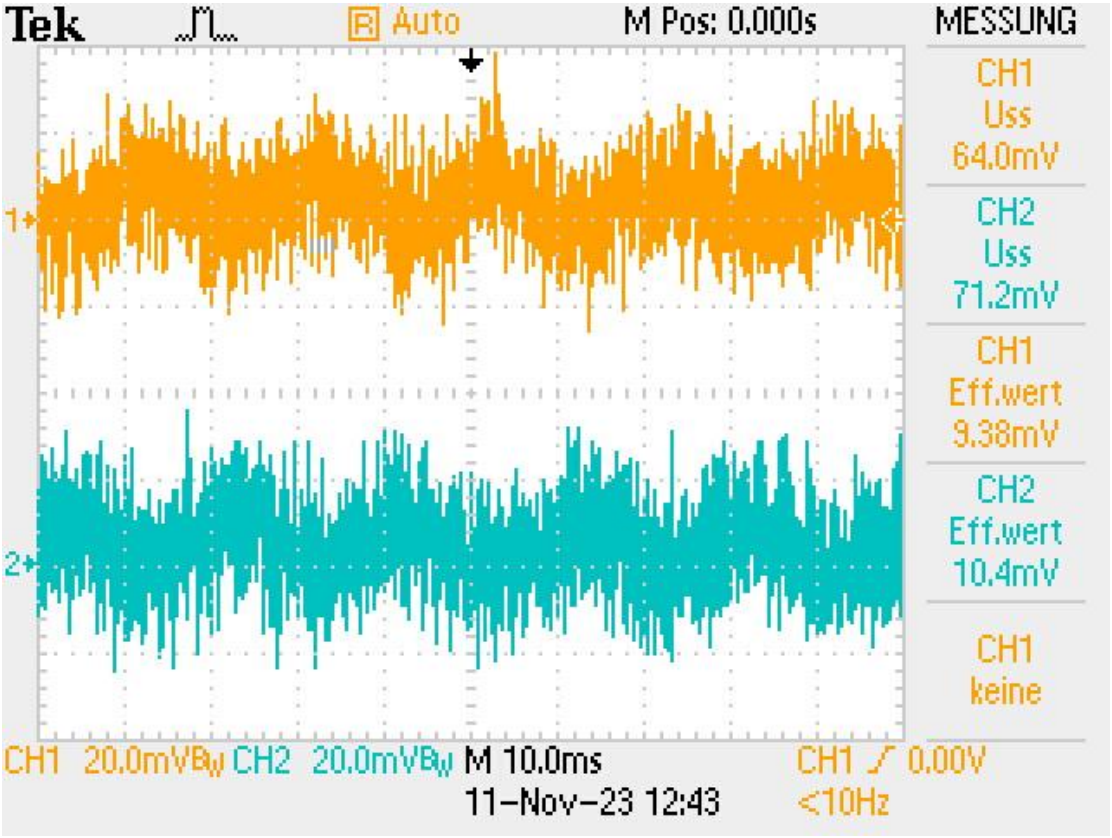

Figure 34: Hall sensor input 5 A at 10 mm

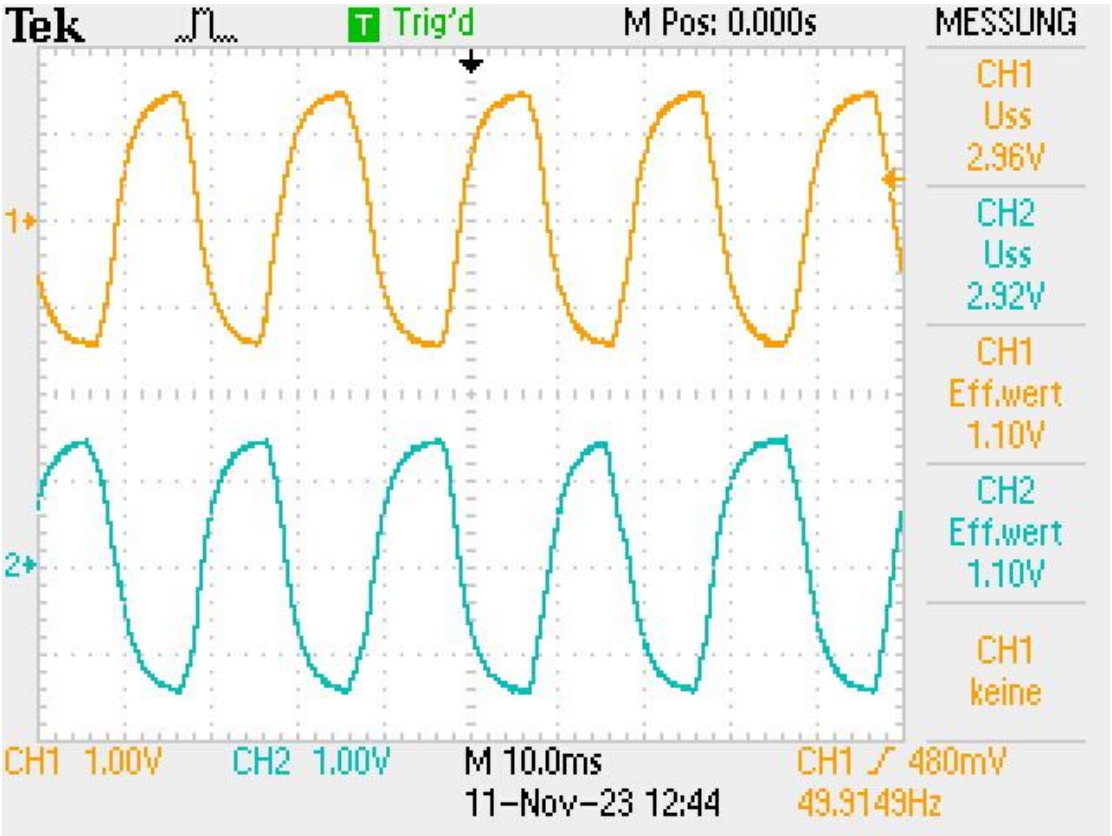

Figure 35: Hall sensor output 5 A at 10 mm